# Changes in latency of brain rhythms in response to affective information of visual stimuli

Yasuki Noguchi*, Sayumi Kubo

*Department of Psychology, Graduate School of Humanities, Kobe University, 1-1 Rokkodai-cho, Nada, Kobe, 657-8501, Japan*

ABSTRACT

It is widely known that emotionally-arousing pictures are perceived more rapidly than non-arousing pictures, although neural underpinnings of this effect remain unclear. Using electroencephalography, we presently measured neural oscillatory rhythms of the human brain in response to various emotional images from the International Affective Picture System. We found that an oscillation frequency in the alpha-to-beta band (8–30 Hz) became higher over the parietal cortex when participants viewed emotionally-arousing than non-arousing pictures. This modulation of neural rhythms was also observed in a valence dimension; emotionally-negative pictures induced faster neural rhythm than emotionally-positive pictures. Those results were consistent with previous studies reporting a speeded perception of high-arousing and negative stimuli (e.g. snakes and spiders) and further provided neural evidence for an adaptive function of emotion to accelerate the processing of potentially-dangerous stimuli.

## 1. Introduction

Mounting evidence indicate that a perception of emotionally-arousing stimuli is faster than non-arousing (neutral) ones. In a visual search task, for example, participants found a target more quickly when it was a fear-relevant picture, such as snakes and spiders, than when the target was a fear-irrelevant picture, such as flowers or mushrooms (Ohman, Flykt, & Esteves, 2001). This facilitated processing of emotional stimuli is thought to be mediated by brain regions showing selective neural responses to affective information, such as the amygdala and nucleus accumbens (Gerdes et al., 2010; Henderson et al., 2012; LeDoux, 2000; Morris, Ohman, & Dolan, 1998). Studies using anatomical- or functional-connectivity analyses further indicated that those subcortical structures were linked with various regions in the cerebral cortex (Pessoa, 2008), forming a whole-brain network for the efficient processing of affective stimuli.

In contrast to the well-defined network of emotional brain regions, it is relatively unknown how affective information changes the temporal profiles of neural activity. Behavioral studies reporting a speeded perception of emotionally-arousing stimuli (Kuhbandner, Spachtholz, & Pastotter, 2016; Ohman et al., 2001) predict that neural activity in the cortical and subcortical regions would be temporally facilitated (accelerated) by affective information. Using a high-temporal resolution of electroencephalography (EEG), a number of studies have tested this

prediction by recording event-related potentials (ERPs) and steady-state visually-evoked potentials (SSVEPs) to emotional pictures. Their results, however, were mixed. Several studies reported the shorter latency of evoked potentials, such as N1 and P2, to emotionally-negative than neutral stimuli (Kemp, Gray, Eide, Silberstein, & Nathan, 2002; Kovalenko, Pavlenko, & Chernyi, 2010; Zhu et al., 2016), while the others not (see Olofsson, Nordin, Sequeira, & Polich, 2008 for an integrative review).

A possible reason for this inconsistency would be the computational procedures of ERPs in which EEG waveforms are directly averaged across trials. Although this approach is effective when neural responses of interest are time-locked to an onset of a stimulus, it is not suitable to detect changes in ongoing or continuous activities (e.g. neural oscillatory signals) that are not necessarily synchronized to the stimulus onset. In the present study, we used a frequency-domain approach and analyzed changes in oscillatory rhythms to emotionally-arousing stimuli. It is well known that waveforms of EEG and magnetoencephalography (MEG) comprise oscillation signals at various frequency bands such as alpha (8–12 Hz), beta (13–30 Hz), and gamma (> 30 Hz) rhythms. Recent studies further indicated that an oscillation frequency of those neural rhythms was closely related to the processing speed of sensory information. For example, individual differences in a peak frequency of alpha rhythm predicted a temporal resolution of one's visual system (Minami & Amano, 2017; Samaha & Postle, 2015). Individuals with a

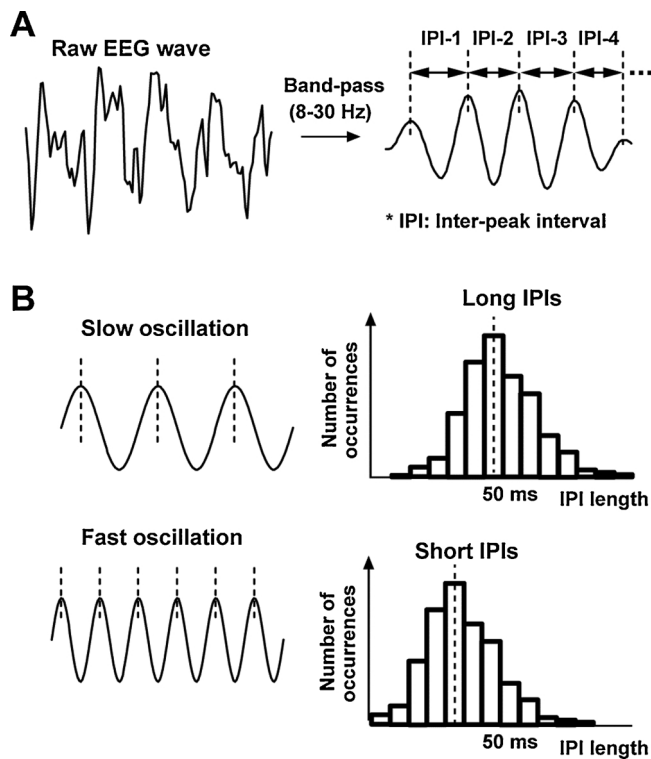**Fig. 1.** Schematic illustrations of the inter-peak interval (IPI) analysis. (A) Band-pass filtering. We first applied a band-pass filter to raw EEG waveforms, extracting oscillatory signals with a frequency band of interest (e.g. 8–30 Hz). A time length between contiguous peaks of the filtered waveform is defined as an IPI. (B) Distributions of IPIs. We pooled all IPIs during a presentation of IAPS images (Fig. 2A) across all trials, depicting a distribution of their occurrences (right panels). Since slow (fast) oscillatory signals produce longer (shorter) IPIs, changes in oscillation frequency can be measured as changes in mean IPIs (vertical dotted lines on IPI distributions).

higher frequency of the alpha rhythm, therefore, can perceive visual stimuli at a higher sampling rate, which facilitates a rapid detection and recognition of those stimuli.

Specifically, we measured emotion-related changes in neural rhythms using the inter-peak interval (IPI) analysis (Noguchi, Xia, & Kakigi, 2019). This analysis first applies a band-pass filter to a raw EEG waveform, extracting oscillatory signals with a frequency band of interest (e.g. 8–30 Hz in Fig. 1A). An IPI is defined as a time interval between neighboring peaks of the filtered waveform. As shown in right panels in Fig. 1B, changes in neural oscillation rhythms can be quantified as a change in mean IPIs. Moreover, the IPI analysis enables us to evaluate the regularity of a brain rhythm (see 2.6 for details). Using this analysis, we previously found a significant reduction of IPIs caused by a spatial allocation of attention (Noguchi et al., 2019); the mean IPI over the left/right visual cortex became shorter when participants attended to a right/left visual field. This attentional modulation of IPIs in a contralateral hemisphere was most clearly observed when we focused on oscillatory signals in alpha-to-beta range (8–30 Hz).

Basic structures of the present EEG study are illustrated in Fig. 2A. Participants viewed a series of affective images taken from the International Affective Picture System or IAPS (Lang, Bradley, & Cuthbert, 2008). Those images consisted of four categories (Fig. 2B) in which two levels of arousal (high/low) are crossed with those of valence (positive/negative). If a frequency of neural oscillations is modulated by affective information, this would be measured as a main effect or interaction of 2-by-2 ANOVA on mean IPIs. In light of the previous studies reporting the speeded perception of affective stimuli (Kuhbandner et al., 2016; Ohman et al., 2001), we predict that a prominent reduction in IPIs would be caused by a presentation of high-arousal & negative pictures
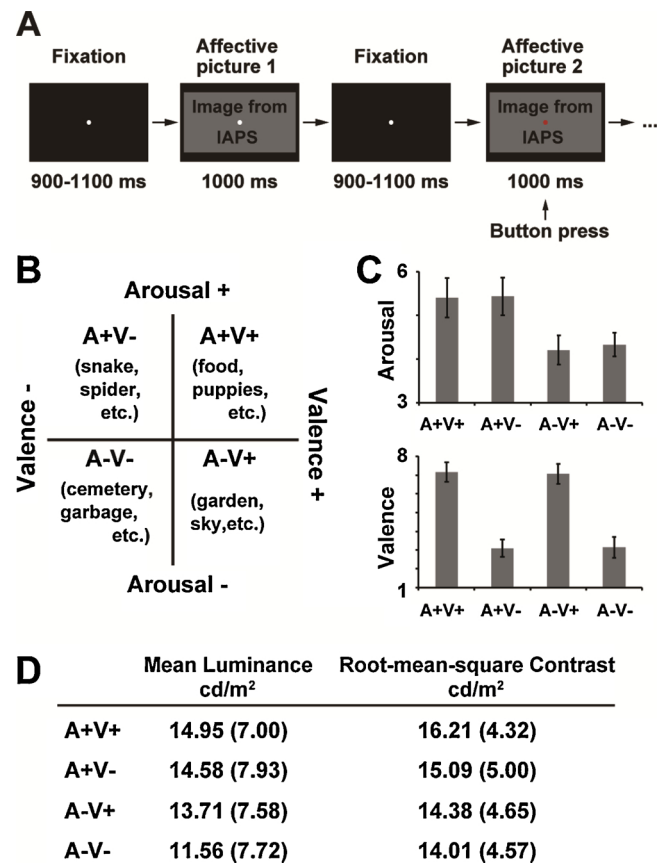


**Fig. 2.** Stimuli and task. (A) Stimulus sequences in an experimental session. Images from IAPS (duration: 1000 ms) were alternately presented with a fixation-only screen (900–1100 ms). Participants pressed a button as quickly as possible when a color of the fixation point over the image changed from white to red (target trials, 12 out of 140). The color change occurred briefly (300 ms), and an interval from an image onset to the color change was randomly set at 100–600 ms. These procedures ensured that participants watched the fixation (and IAPS image) continuously until the end of an image screen. (B) Four groups of affective pictures (32 images per group) in non-target trials. High-arousal positive images are expressed as A + V + , while low-arousal negative images are expressed as A − V − . (C) Scores of arousal and valence ratings for 128 pictures used in the present study. These scores are taken from the normative IAPS database (Lang et al., 2008) (D) Data of mean luminance and root-mean-square contrast for the four image groups. Standard deviations across 32 images are shown in parentheses. A two-way ANOVA of arousal (+/−) × valence (+/−) on each measure indicated no main effect or interaction (see text for details).

(e.g. snakes and spiders) because of a potential threat conveyed by those images (LeDoux, 2000; Morris, Ohman, & Dolan, 1999).

## 2. Methods

### 2.1. Participants

Thirty-seven healthy subjects (18 females, age: 18–24) participated in the present study. Data of three subjects were excluded from analyses because of an excessive noise in EEG waveforms and a technical problem in measurements. All results below were thus obtained from the data of remaining 34 participants. This sample size was based on the power analysis using G*Power 3 (Faul, Erdfelder, Lang, & Buchner, 2007). The type I error rate (alpha) and statistical power (1 - beta) were set at 0.05 and 0.80, respectively. An effect size was assumed to be middle and set at 0.5 (Cohen, 1988), because no previous study has measured emotion-related changes in IPIs. Informed consent was received from each participant after the nature of the study had been

explained. All experiments were carried out in accordance with guidelines and regulations approved by the ethics committee of Kobe University, Japan.

### 2.2. Stimuli and task

Visual stimuli were generated with the Psychophysics Toolbox on Matlab (Brainard, 1997; Pelli, 1997) and presented on a CRT monitor at a refresh rate of 75 Hz. In each experimental session, we sequentially presented 140 images from the IAPS (size: 10.24 × 7.68 deg, duration: 1000 ms for each) with a white fixation point (0.12 × 0.12 deg) at the center of images (Fig. 2A). Each image was followed by a fixation-only screen with a black background (inter-trial interval, 900–1100 ms). In 12 out of 140 trials, a color of the fixation point changed from white to red briefly (300 ms). Participants pressed a button as fast as possible when they detected the red fixation point (target trials). An interval from an onset of an image screen to the color change was randomly set at 100–600 ms, so that participants had to watch the fixation point (and IAPS image) continuously until the end of the screen.

Images in 128 non-target trials were composed of four groups (32 images for each) produced by a combination of arousal (high/low) and valence (positive/negative) factors. As shown in Fig. 2B, high-arousal positive stimuli are expressed as $A+V+$, while low-arousal negative stimuli are expressed as $A-V-$. Each participant underwent two experimental sessions of 140 trials in which the 128 affective images were randomly intermixed with 12 target trials.

Previous studies indicated that neural activity related to the processing of affective information can be observed in both passive viewing and active response tasks (Olofsson et al., 2008). Differences in EEG responses across the four conditions ($A+V+$, $A+V-$, $A-V+$, and $A-V-$) thus would reflect differences in arousal and valence levels of IAPS images.

### 2.3. Images from IAPS

Slide numbers of the 140 IAPS images are shown in Table S1 in Supplementary Materials. Rating scores of arousal and valence for those images are available in technical manual of IAPS (Lang et al., 2008) and summarized in Fig. 2C. A two-way ANOVA of arousal ($+/-$) × valence ($+/-$) on the arousal scores (upper panel of Fig. 2C) indicated a significant main effect of arousal ($A+V+$ and $A+V- > A-V+$ and $A-V-$, $F(1,124) = 290.67$, $p < 0.001$, $\eta^2 = 0.701$) but not a main effect of valence ($F(1,124) = 1.36$, $p = 0.25$, $\eta^2 = 0.011$) or an interaction ($F(1,124) = 0.45$, $p = 0.50$, $\eta^2 = 0.004$). An ANOVA on the valence scores (lower panel of Fig. 2C) indicated a significant main effect of valence ($A+V+$ and $A-V+ > A+V-$ and $A-V-$, $F(1,124) = 1892.24$, $p < 0.001$, $\eta^2 = 0.938$) but not a main effect of arousal ($F(1,124) = 0.02$, $p = 0.88$, $\eta^2 < 0.001$) or an interaction ($F(1,124) = 0.59$, $p = 0.44$, $\eta^2 = 0.005$).

To equalize low visual features of images across the four groups, we changed luminance and contrast of some IAPS pictures using image-editing software. Mean luminance and root-mean-square (RMS) contrast after the change are shown in Fig. 2D. A two-way ANOVA of arousal ($+/-$) × valence ($+/-$) on the mean luminance indicated no main effect or interaction ($F(1,124) < 2.56, p > 0.11, \eta^2 < 0.020$). An ANOVA on the RMS contrast indicated no main effect or interaction ($F(1,124) < 3.12, p > 0.08, \eta^2 < 0.024$).

### 2.4. EEG recordings

We recorded EEG waveforms from 32 points over the scalp (FP1, FP2, AF3, AF4, F7, F3, Fz, F4, F8, FC5, FC1, FC2, FC6, T7, C3, Cz, C4, T8, CP5, CP1, CP2, CP6, P7, P3, Pz, P4, P8, PO3, PO4, O1, Oz, and O2) using the ActiveTwo system by Biosemi (Amsterdam, Netherlands). Those signals were measured with an analog low-pass filter of 417 Hz at a sampling rate of 2048 Hz. The preprocessing of EEG data was

performed with the Brainstorm toolbox for Matlab (Tadel, Baillet, Mosher, Pantazis, & Leahy, 2011). First, a fixed-frequency noise from power line (60, 120, and 180 Hz) was removed with a notch filter. We then applied a band-pass filter of 0.5–200 Hz to eliminate low and high frequency noises. Noises caused by eye blinks were also identified and excluded with the ICA (independent component analysis) decomposition in the Brainstorm. All EEG data were then re-referenced with an average potential across the 32 electrodes.

Finally, EEG waveforms were segmented and classified into five conditions ($A+V+$, $A+V-$, $A-V+$, $A-V-$, and target). An epoch for the segmentation ranged from $-1000$ to 1799.8 ms relative to an onset of an IAPS image. Trials in which a signal variation (a max-min difference within a period of $-200.2$ to 1000 ms) was larger than 100 μV were excluded from analyses. We also discarded data of the target trials, because waveforms in those trials contained noises emerging from manual button-press movements.

### 2.5. Time-frequency power analysis

Changes in powers of oscillatory signals were measured by the time-frequency (TF) decomposition with complex Morlet wavelets (central frequency: 1 Hz, time resolution at full width at half maximum: 3 s). This method converted the segmented EEG waveforms into power spectra of time ($-1000$ to 1799.8 ms) × frequency (1 to 100 Hz). Those TF spectra were then averaged across trials at each electrode position. Finally, we performed a baseline correction of the TF data. For each frequency, all data from $-1000$ to 1799.8 ms were converted into decibel (dB) change from a baseline (Fig. 3), as shown by an equation below.

$$y = 10 \times \log_{10}(x/u)$$

The $x$ and $y$ indicate powers before and after the baseline correction, and $u$ indicates a mean power over a pre-stimulus baseline period ($-200.2$ to 0 ms).

### 2.6. IPI analysis

Changes in oscillation frequency were measured by the IPI (inter-peak interval) analysis. First, we applied a band-pass filter to the segmented EEG waveforms in each trial. A pass-band of the filter was set at alpha-to-beta range (8–30 Hz) based on our previous study (Noguchi et al., 2019). Peaks of the filtered waveform were then identified using the Matlab findpeaks.m function. No amplitude threshold was used to define those peaks. We measured each IPI as an interval between neighboring peaks. The IPIs within a time window of 200–1000 ms were analyzed in the present study (see a dotted rectangle in Fig. 4A), because EEG waveforms from 0 to 200 ms contained low-frequency components of visual-evoked potentials (e.g. P100 and N170). Finally, we computed a mean length of IPIs pooled across all trials in a given condition (e.g. $A+V+$). As shown in Fig. 1B, a slower oscillatory signal produces longer IPIs (upper panels) while faster one produces shorter IPIs (lower panels). Changes in neural oscillation rhythms can be thus quantified as a change in mean IPIs (a horizontal shift of a distribution of IPIs, right panels in Fig. 1B).

A hallmark of the IPI analysis is that it can evaluate not only a frequency but also the regularity of a brain rhythm by calculating a standard deviation (SD) of an IPI distribution (Noguchi et al., 2019). When a rhythm is highly regular (periodic), most IPIs would be located around a center (mean) of the distribution, which leads to a smaller SD. In contrast, an irregular rhythm would be characterized by a large SD because such irregular rhythm produces IPIs far from the mean. As a supplementary analysis, we investigated how affective factors in visual stimuli influenced the regularity of oscillatory signals at 8–30 Hz.
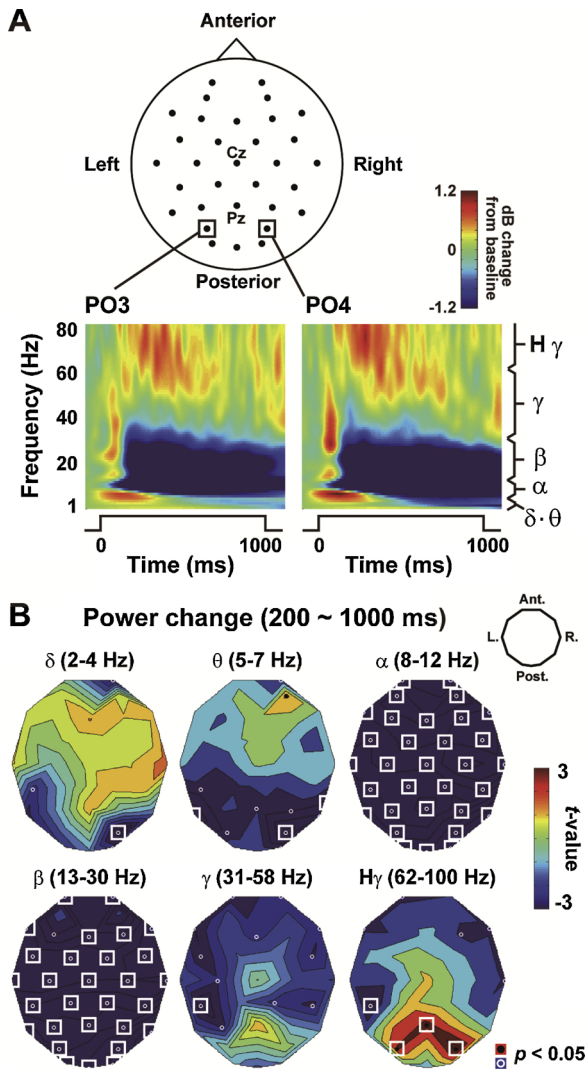
**Fig. 3.** Perceptual (visually-induced) decreases in powers of oscillation signals. (A) A two-dimensional layout of 32 EEG electrodes (upper panel) and time-frequency (TF) power spectra at PO3 and PO4 (lower panels) in A + V + trials. A presentation of visual stimulus induced a prominent decrease in alpha (8–12 Hz) and beta (13–30 Hz) powers starting at around 200 ms after the stimulus onset. (B) Statistical *t*-maps of power changes. For each of six bands from delta (2–4 Hz) to high-gamma (62–100 Hz), mean oscillatory power in a stimulus presentation period (200 to 1000 ms) was compared with that in a pre-stimulus baseline period (−500 to 0 ms). Resultant *t*-values are color-coded over the layout of 32 electrodes (*t*-values at anterior electrodes are shown in upper positions on the map). Black dots and white circles indicate electrodes with a significant ($p < 0.05$, uncorrected) difference. Electrode positions with a significant difference after the correction of multiple comparisons are indicated by white rectangles. The visually-induced power decreases (pre-stimulus > post-stimulus, colored in blue) were widely observed in alpha and beta bands.

### 2.7. Instantaneous frequency (IF) analysis

We also computed instantaneous frequency (Cohen, 2014; Wutz, Melcher, & Samaha, 2018) of alpha-to-beta rhythm, as another index for a speed of neural oscillation. First, EEG signals at 8–30 Hz were isolated with the band-pass filter above. We then applied the Hilbert transform to the filtered waveform, extracting changes in phase angle over time. The instantaneous frequency (IF) was defined as the temporal derivative of this phase-angle time series scaled by a sampling rate and 2*pi. Noises in the instantaneous-frequency waveforms were removed by a median filter with 11 equally-spaced time windows from
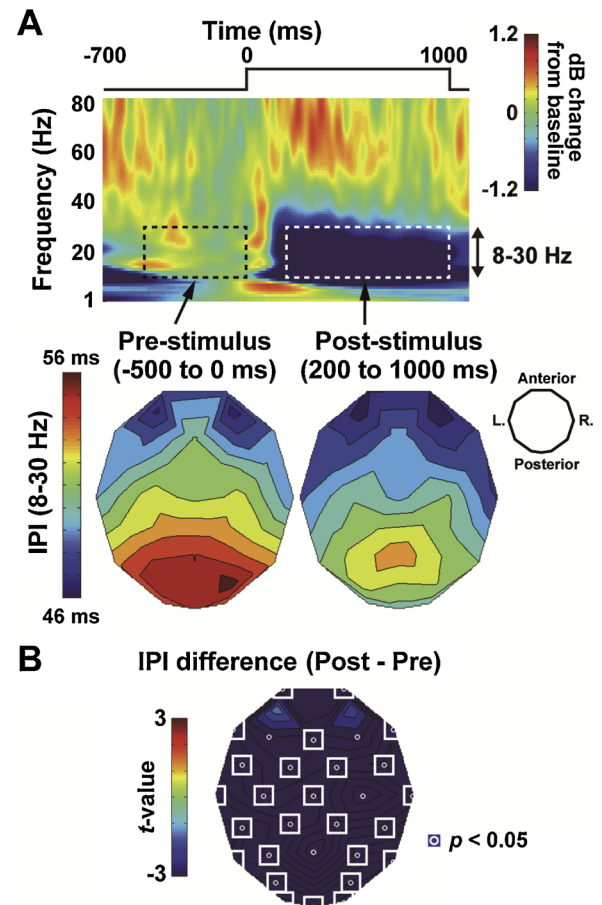


**Fig. 4.** Visually-induced decreases in mean IPIs. (A) TF power spectrum at PO3 (identical to Fig. 3A) and contour maps of mean IPIs in a pre-stimulus (lower left) and post-stimulus (lower right) periods. A band-pass filter for the IPI analysis was set at 8–30 Hz (alpha-to-beta band, as shown by the dotted rectangles in the TF spectrum). (B) A *t*-map of mean IPIs between the pre-stimulus and post-stimulus periods. Visually-induced reductions of IPIs ($p < 0.05$ corrected, indicated by white rectangles) were seen at almost all electrodes. Neural oscillatory signals in 8–30 Hz were therefore suppressed in amplitude (Fig. 3) but accelerated temporally by a presentation of visual stimuli.

10 to 410 ms. A median across the 11 filtered waveforms was selected to estimate the instantaneous frequency at each time point. These procedures were repeated for each trial, condition, and participant.

### 2.8. Statistical procedures

Statistical comparisons were made on the mean powers and IPIs at the time window of 200–1000 ms. First, we investigated changes in powers induced by a presentation of IAPS images (visually-induced changes in powers, see 3.2.). At each of 32 electrodes, mean oscillatory power in a post-stimulus period (200 to 1000 ms) was compared with that in a pre-stimulus period (−500 to 0 ms) in a given condition (e.g. A + V +). Resultant *t*-maps over the 32 electrodes were shown in Fig. 3B. An issue of multiple comparisons (caused by a repetition of *t*-test at 32 positions) was resolved by a non-parametric approach (Groppe, Urbach, & Kutas, 2011). Through random permutations of original data for 1,000 times, we generated a distribution of maximum *t*-value across the 32 positions under a hypothesis of null effect. A significance threshold was determined as 5-% tail of this null distribution. A change in TF powers was considered as significant only when the *t*-value obtained from actual data exceeded this threshold.

We then investigated the changes in mean powers induced by emotional factors (*3.6. Emotion-related changes in oscillatory powers* and
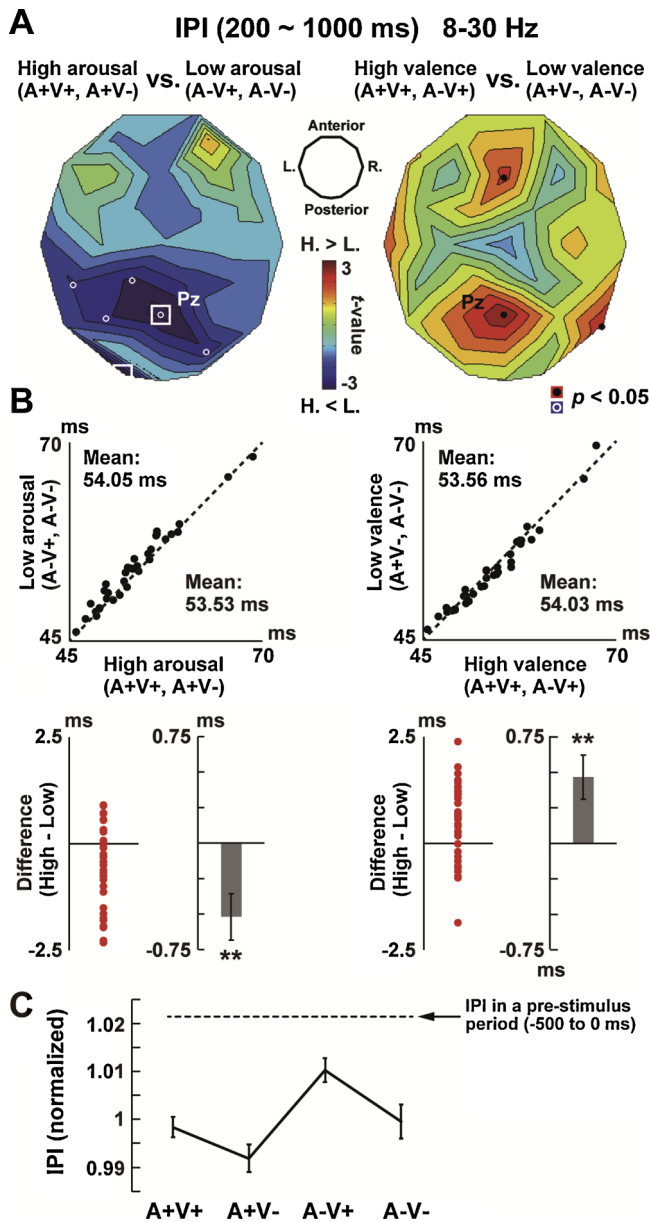
**Fig. 5.** Emotion-related changes in IPIs. (A) *t*-maps of IPI (8–30 Hz) at 200–1000 ms. Mean IPIs in high-arousal condition (average of A + V + and A + V −) were shorter than those in low-arousal (average of A − V + and A − V −) conditions (arousal effect, left panel). The Pz electrode also showed a valence effect (right panel) in which mean IPIs in high-valence condition (average of A + V + and A − V +) were longer than those in low-valence (average of A + V − and A − V −) conditions. (B) Mean IPIs of individual subjects at Pz. In the left panel (arousal effect), individual data (N = 34, black dots) in high-arousal (*x*) and low-arousal (*y*) conditions are shown on two-dimensional plots with 45-deg line. Red dots in the lower panel denote between-condition differences (high – low) with their mean ± SE shown as the bar graph. Comparisons between positive and negative conditions (valence effect) are made in right panels. ** *p* < 0.01. (C) Emotion-related changes in IPIs (200–1000 ms, mean ± SE) in all four conditions. The mean IPI in a pre-stimulus period (−500 to 0 ms) is also shown as dotted line. To correct for an inter-individual difference in IPI lengths, all data are normalized to the mean across the four conditions in each participant. The most prominent decrease in IPIs was observed when participants viewed high-arousal & negative stimuli (A + V −).

Fig. 6). At each of 32 electrodes, an effect of arousal was tested by a paired *t*-test (N = 34 vs. 34) between high-arousal conditions (average of A + V + and A + V −) and low-arousal conditions (average of A − V +
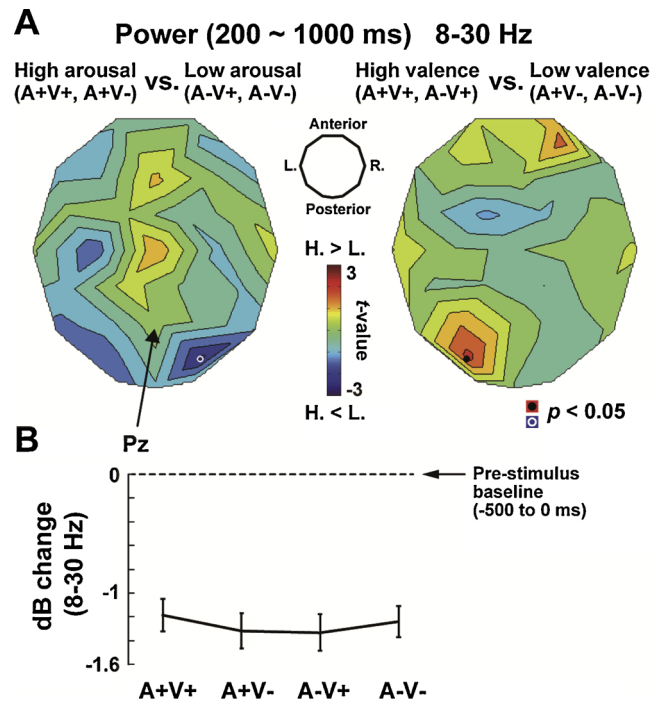


**Fig. 6.** Emotion-related changes in oscillatory powers. (A) *t*-maps for the arousal effect (left) and valence effect (right). (B) Changes in oscillatory powers (200–1000 ms) at Pz. The dB changes from a pre-stimulus baseline are shown. No systematic change was observed across the four conditions.

and A − V −). An effect of valence was tested by contrasting mean powers between high-valence (positive) conditions (average of A + V + and A − V +) and low-valence (negative) conditions (average of A + V − and A − V −). The problem of multiple comparisons was resolved by the permutation approach described above.

Those statistical procedures on power analyses were also used for analyses on IPIs. Changes in mean IPIs induced by the presentation of IAPS images (pre-stimulus vs. post-stimulus periods) are shown in Fig. 4, while those related to emotional factors are shown in Fig. 5. Regarding the IF, we focused on electrodes at which significant effects of emotional factors were observed in the IPI analyses, because a purpose of the IF analyses was to confirm its consistency with the IPI analyses.

### 2.9. Post-experimental ratings of affective pictures

After measuring EEG data, we asked participants to rate arousal and valence of the IAPS images. The 128 pictures that had been presented in EEG sessions were shown again on the CRT monitor, in a different presentation order from the EEG sessions. Participants judged the arousal level of each picture using a 5-point scale from 1 (calm) to 5 (exciting). They also provided the valence score for the same picture using the scale from 1 (unpleasant) to 5 (pleasant). No time limitation was imposed on these rating tasks.

## 3. Results

### 3.1. Behavioral data

Hit and false-alarm rates for the color change of a fixation point were 97.92 ± 0.66% and 0.20 ± 0.05%, respectively (mean ± SE across participants). A reaction time measured from an onset of the change was 546.06 ± 10.64 ms. These data ensured that participants attended to the fixation point continuously during a presentation of the IAPS images.

Arousal scores in the post-experimental rating task were $3.32 \pm 0.08$ (A+V+), $3.90 \pm 0.08$ (A+V−), $2.59 \pm 0.08$ (A−V+), and $2.95 \pm 0.07$ (A−V−). A planned comparison between high-arousal conditions (A+V+ and A+V−) and low-arousal conditions (A−V+ and A−V−) yielded a significant difference ($t(67) = 16.6$, $p < 0.001$, Cohen's $d = 1.65$). Valence scores were $4.15 \pm 0.07$ (A+V+), $1.53 \pm 0.06$ (A+V−), $4.15 \pm 0.07$ (A−V+), and $1.79 \pm 0.05$ (A−V−). A planned comparison between high-valence conditions (A+V+ and A−V+) and low-valence conditions (A+V− and A−V−) yielded a significant difference ($t(67) = 32.3$, $p < 0.001$, Cohen's $d = 6.52$). These data confirmed that affective information in the original IAPS images was preserved in the present study.

### 3.2. Visually-induced changes in powers

Fig. 3A shows TF power spectra (averaged across 34 participants) at PO3 and PO4 in A+V+ condition. A presentation of visual stimuli induced an increase in power (event-related synchronization or ERS) from delta (2–4 Hz) to gamma (31–58 Hz) bands at 0–200 ms. This was followed by a prominent power decrease (event-related desynchronization or ERD) in alpha (8–12 Hz) and beta (13–30 Hz) bands at 200–1000 ms. Fig. 3B shows *t*-maps showing the visually-induced ERDs. For each of six frequency bands from delta to high-gamma (62 to 100 Hz), mean power in a pre-stimulus period (−500 to 0 ms) was compared with that in a post-stimulus period (200–1000 ms). Significant ERD in alpha and beta rhythms (pre > post, colored in blue) was observed at almost all electrodes ($p < 0.05$, corrected for multiple comparisons). We also found the visually-induced ERS in high-gamma band (lower right panel in Fig. 3B), which was consistent with many previous studies using visual stimuli (Gunduz et al., 2011; Wyart & Tallon-Baudry, 2008). Although we showed the data of A+V+ in Fig. 3, similar changes in powers were also seen in the other conditions (A+V−, A−V+, and A−V−), indicating that those reflected perceptual (not emotional) changes in oscillatory signals.

### 3.3. Visually-induced changes in IPIs

Our previous study (Noguchi et al., 2019) has shown that the visually-induced ERD in alpha and beta bands involved a significant reduction of IPIs in the same frequency range. We checked a reproducibility of this effect (perceptual reduction of IPIs) using the present data. Fig. 4A shows contour maps of mean IPIs in the alpha-to-beta band (8–30 Hz) at pre-stimulus (lower left) and post-stimulus (lower right) periods. A statistical comparison between pre- and post-stimulus data revealed significant changes of IPIs (pre > post) at almost all electrodes (Fig. 4B). Neural oscillations at 8–30 Hz were thus not only suppressed in amplitudes (Fig. 3) but also became faster (Fig. 4) by a presentation of visual stimuli.

### 3.4. Emotion-related changes in IPIs

We next investigated how the affective information in the IAPS pictures modulated a frequency of brain rhythms. Fig. 5A shows *t*-maps for effects of arousal (left panel) and valence (right panel) on mean IPIs at 200–1000 ms. Oscillatory signals in alpha-to-beta band showed shorter IPIs in high-arousal conditions (A+V+ and A+V−) than low-arousal conditions (A−V+ and A−V−). Significant reductions in IPIs after the correction of multiple comparisons were observed at Pz and O1 (left panel). The oscillation frequency at Pz was also modulated by valence of stimuli (right panel); the IPIs in high-valence conditions (A+V+ and A−V+) were significantly longer than those in low-valence conditions (A+V− and A−V−).

Individual data of mean IPIs at Pz are shown in Fig. 5B. In the left panel (arousal effect), most black dots were located above a diagonal (45-deg) line, indicating that IPIs in high-arousal conditions (abscissa) were shorter than those in low-arousal conditions (ordinate).

Differences of mean IPI (high – low) were thus negative in most participants (red dots). These patterns were reversed in the right panels (valence effect) in which mean IPI was longer in high-valence than low-valence conditions.

Fig. 5C displays mean IPIs at Pz separately shown for the four conditions. Although the visually-induced reduction of IPIs was evident in all conditions, the most prominent one was seen in A+V− condition where high-arousal & negative pictures were presented. A repeated measures ANOVA of arousal (+/−) × valence (+/−) indicated significant main effects of arousal ($F(1,33) = 10.47$, $p = 0.0028$, $\eta^2 = 0.241$) and valence ($F(1, 33) = 9.07$, $p = 0.005$, $\eta^2 = 0.216$), but not an interaction ($F(1, 33) = 0.43$, $p = 0.52$, $\eta^2 = 0.013$). This lack of interaction was also seen at other electrodes, as shown by topographical *F*-maps in Fig. S1 in Supplementary Materials.

We also showed results of the IF (instantaneous frequency) analysis in Fig. S2. Consistent with the IPI analysis, our data showed significant modulation of IF in posterior brain regions across the four conditions. Statistical comparisons across the four conditions were made using an average between the two electrodes (Pz and O1) where the emotion-related changes in IPIs were significant. A repeated measures ANOVA of arousal (+/−) × valence (+/−) on mean instantaneous frequency at 200–1000 ms indicated significant main effects of arousal ($F(1,33) = 15.13$, $p < 0.001$, $\eta^2 = 0.314$) and valence ($F(1, 33) = 6.95$, $p = 0.013$, $\eta^2 = 0.174$), but not an interaction ($F(1, 33) = 1.01$, $p = 0.32$, $\eta^2 = 0.030$).

### 3.5. Emotion-related changes in regularity of brain rhythms

A hallmark of the IPI analysis is that it can evaluate the regularity of oscillatory signals by measuring the SD of an IPI distribution (*2.6.*). Specifically, we used an index called the coefficient of variation (CV) (Softky & Koch, 1993; Taube, 2010), which is the SD normalized to (divided by) the mean IPI. A smaller CV denotes higher regularity (lower SD) of a brain rhythm (Noguchi et al., 2019). Results of statistical comparisons of CVs across the four conditions are shown in Fig. S3. Although we observed some changes in CVs by arousal and valence factors, these changes did not reach significance. These results indicate that affective factors did *not* modulate the regularity of brain rhythms.

### 3.6. Emotion-related changes in oscillatory powers

Fig. 6 shows emotion-related changes in power of the alpha-to-beta band at 200–1000 ms. Although data at some electrodes showed increase and decrease in powers (Fig. 6A), no change was observed at Pz (Fig. 6B). A repeated measures ANOVA of arousal (+/−) × valence (+/−) indicated no main effect (arousal: $F(1, 33) = 0.18$, $p = 0.67$, $\eta^2 = 0.005$, valence: $F(1, 33) = 0.11$, $p = 0.74$, $\eta^2 = 0.003$) or interaction ($F(1, 33) = 2.70$, $p = 0.11$, $\eta^2 = 0.076$).

## 4. Discussion

We presently measured changes in oscillation frequency of neural rhythms in response to various types of affective pictures. Consistent with a previous study (Noguchi et al., 2019), mean IPIs in alpha-to-beta band (8–30 Hz) were significantly reduced during a presentation of visual stimuli (perceptual reduction of IPIs, Fig. 4). Comparisons across the four groups of affective images (Fig. 5) further showed that IPIs became shorter when participants viewed high-arousal than low-arousal images (the arousal effect) and when they viewed negative than positive images (the valence effect).

One possible reason for those changes in mean IPIs is the contamination of EEG data by electromyographic (EMG) activity. For example, presenting pictures of A+V− (e.g. snakes) might induce muscle contractions of participants. The EMG activity caused by the contraction might change peak frequency of EEG signals, thereby producing shorter IPIs in A+V− than the other three conditions. To examine this

possibility, we re-analyzed our data by focusing on powers and mean IPIs at around 10 Hz and 20 Hz (Fig. S4). Previous studies have reported that typical EMG activity has several discrete peaks in a frequency domain at 10, 20, and 40 Hz (Goncharova, McFarland, Vaughan, & Wolpaw, 2003; McAuley, Rothwell, & Marsden, 1997). If the emotion-related changes in IPIs (Fig. 5) resulted from the contamination by EMG signals, those changes would be observed more clearly when we focus on frequency bands at which the EMG signals are prominent (such as 8–12 Hz and 18–22 Hz). Results of the power analysis are shown in Fig. S4A and those of the IPI analysis are shown in Fig. S4B. In both analyses, we found no significant change that can explain the emotion-related effects in IPIs (Fig. 5). Those data suggest that the present EEG results were not seriously contaminated by the EMG activity.

The present results of the IPI analysis were consistent with previous studies measuring behavioral responses to affective stimuli. Emotionally-negative words are generally processed faster and more efficiently than positive words (Dijksterhuis & Aarts, 2003; Kuhbandner et al., 2016; Nasrallah, Carmel, & Lavie, 2009). Some studies also reported a speeded perception of high-arousal & negative stimuli (Hofmann, Kuchinke, Tamm, Vo, & Jacobs, 2009; Ohman et al., 2001). Our data went along with those studies and further provided neural evidence that oscillatory rhythms at the Pz were modulated by both arousal and valence of stimuli. The Pz is one of the typical electrode positions where emotion-related changes in EEG signals were detected (Brazdil et al., 2009; Lu, Jaquess, Hatfield, Zhou, & Li, 2017; Mini, Palomba, Angrilli, & Bravi, 1996), and it is located over a core region of the front-parietal attention network (Corbetta & Shulman, 2002). The IPI changes in the present study might support an adaptive function of emotion to orient attention rapidly into a high-arousal & negative stimulus that is frequently associated with potential danger to life (LeDoux, 2000; Morris et al., 1999).

It is also notable that those changes in IPIs were observed even when affective pictures were presented as distractors. As described in *2.2. Stimuli and task*, participants detected a color change of a fixation point randomly taking place in a subset of trials. This procedure would guide attention of participants to the fixation point, making the IAPS images task-irrelevant distractors. The changes in mean IPIs thus might represent an automatic (reflexive) shift of attention by emotional factors that was difficult to inhibit by voluntary control.

Finally, we admit that there are several limitations of the present study. The first limitation was a lack of control condition in which emotionally-neutral images are presented as non-target stimuli. Although our data predict that those neutral stimuli would produce IPIs with an average length across the four conditions (A + V+, A + V−, A − V+, and A − V−), this prediction should be tested in future studies. Second, a spatial resolution of scalp EEG is limited because of volume conduction of electrical signals in the cerebrospinal fluid layer. Since we did not use sophisticated methods to estimate anatomical source locations, topographical effects on the scalp as a cortex activity (e.g. *t*-maps over the layout of 32 electrodes) should be interpreted cautiously. Third, we presented affective images as task-irrelevant distractors, using the detection task of a color change over a fixation point. Although this task was a unique point in the present study (see above), it also made a comparison of the present study with previous ones difficult. For example, we found no emotion-related change in oscillatory powers in the present study (*3.6*). In contrast, a number of studies have reported emotion-related changes of powers in delta (Balconi, Brambilla, & Falbo, 2009; Klados et al., 2009), theta (Balconi et al., 2009), beta (Guntekin & Basar, 2010; Woodruff, Barbera, & Von Oepen, 2016), and gamma bands (Keil et al., 2001; Martini et al., 2012; Muller, Keil, Gruber, & Elbert, 1999; Oya, Kawasaki, Howard, & Adolphs, 2002). One of those studies further reported an interaction between arousal and valence factors (Klados et al., 2009), whereas no interaction was observed in the present IPI data (*3.4*). These inconsistencies between present and previous results might partly emerge from differences in tasks. In many previous studies above, participants passively

viewed affective images or they evaluated arousal and valence of images. In other words, participants can fully attend to affective images. In contrast, IAPS pictures were shown as task-irrelevant distractors in the present study. This lack of voluntary (top-down) attention to affective images might obscure emotion-related changes in powers that had been reported by the previous studies.

## Declaration of Competing Interest

The authors declare that they have no known competing financial interests or personal relationships that could have appeared to influence the work reported in this paper.

## Acknowledgment

## Appendix A. Supplementary data

Supplementary material related to this article can be found, in the online version, at doi:https://doi.org/10.1016/j.biopsycho.2019.107787.

## References

Balconi, M., Brambilla, E., & Falbo, L. (2009). BIS/BAS, cortical oscillations and coherence in response to emotional cues. *Brain Research Bulletin, 80*(3), 151–157.

Brainard, D. H. (1997). The psychophysics toolbox. *Spatal Vision, 10*(4), 433–436.

Brazdil, M., Roman, R., Urbanek, T., Chladek, J., Spok, D., Marecek, R., et al. (2009). Neural correlates of affective picture processing–a depth ERP study. *Neuroimage, 47*(1), 376–383.

Cohen, J. (1988). *Statistical power analysis for the behavioral sciences* (2nd ed.). Hillsdale, N.J: L. Erlbaum Associates.

Cohen, M. X. (2014). Fluctuations in oscillation frequency control spike timing and coordinate neural networks. *Journal of Neuroscience, 34*(27), 8988–8998.

Corbetta, M., & Shulman, G. L. (2002). Control of goal-directed and stimulus-driven attention in the brain. *Nature Reviews Neuroscience, 3*(3), 201–215.

Dijksterhuis, A., & Aarts, H. (2003). On wildebeests and humans: The preferential detection of negative stimuli. *Psychological Science, 14*(1), 14–18.

Faul, F., Erdfelder, E., Lang, A. G., & Buchner, A. (2007). G*Power 3: A flexible statistical power analysis program for the social, behavioral, and biomedical sciences. *Behavior Research Methods, 39*(2), 175–191.

Gerdes, A. B., Wieser, M. J., Muhlberger, A., Weyers, P., Alpers, G. W., Plichta, M. M., et al. (2010). Brain activations to emotional pictures are differentially associated with Valence and arousal ratings. *Frontiers in Human Neuroscience, 4*, 175.

Goncharova, I. I., McFarland, D. J., Vaughan, T. M., & Wolpaw, J. R. (2003). EMG contamination of EEG: Spectral and topographical characteristics. *Clinical Neurophysiology, 114*(9), 1580–1593.

Groppe, D. M., Urbach, T. P., & Kutas, M. (2011). Mass univariate analysis of event-related brain potentials/fields I: A critical tutorial review. *Psychophysiology, 48*(12), 1711–1725.

Gunduz, A., Brunner, P., Daitch, A., Leuthardt, E. C., Ritaccio, A. L., Pesaran, B., et al. (2011). Neural correlates of visual-spatial attention in electrocorticographic signals in humans. *Frontiers in Human Neuroscience, 5*, 89.

Guntekin, B., & Basar, E. (2010). Event-related beta oscillations are affected by emotional eliciting stimuli. *Neuroscience Letters, 483*(3), 173–178.

Henderson, L. A., Stathis, A., James, C., Brown, R., McDonald, S., & Macefield, V. G. (2012). Real-time imaging of cortical areas involved in the generation of increases in skin sympathetic nerve activity when viewing emotionally charged images. *Neuroimage, 62*(1), 30–40.

Hofmann, M. J., Kuchinke, L., Tamm, S., Vo, M. L., & Jacobs, A. M. (2009). Affective processing within 1/10th of a second: High arousal is necessary for early facilitative processing of negative but not positive words. *Cognitive, Affective & Behavioral Neuroscience, 9*(4), 389–397.

Keil, A., Muller, M. M., Gruber, T., Wienbruch, C., Stolarova, M., & Elbert, T. (2001). Effects of emotional arousal in the cerebral hemispheres: A study of oscillatory brain activity and event-related potentials. *Clinical Neurophysiology, 112*(11), 2057–2068.

Kemp, A. H., Gray, M. A., Eide, P., Silberstein, R. B., & Nathan, P. J. (2002). Steady-state visually evoked potential topography during processing of emotional valence in healthy subjects. *Neuroimage, 17*(4), 1684–1692.

Klados, M. A., Frantzidis, C., Vivas, A. B., Papadelis, C., Lithari, C., Pappas, C., et al. (2009). A framework combining delta Event-Related Oscillations (EROs) and Synchronisation Effects (ERD/ERS) to study emotional processing. *Computational Intelligence and Neuroscience*549419.

Kovalenko, A. A., Pavlenko, V. B., & Chernyi, S. V. (2010). Reflection of the emotional

significance of visual stimuli in the characteristics of evoked EEG potentials. *Neurophysiology, 42*(1), 70–79.

Kuhbandner, C., Spachtholz, P., & Pastotter, B. (2016). Bad things come easier to the mind but harder to the body: Evidence from brain oscillations. *Cognitive, Affective & Behavioral Neuroscience, 16*(4), 768–778.

Lang, P. J., Bradley, M. M., & Cuthbert, B. N. (2008). *International affective picture system (IAPS): Affective ratings of pictures and instruction manual*Technical Report A-8. Gainesville, FL: University of Florida.

LeDoux, J. E. (2000). Emotion circuits in the brain. *Annual Review of Neuroscience, 23*, 155–184.

Lu, Y., Jaquess, K. J., Hatfield, B. D., Zhou, C., & Li, H. (2017). Valence and arousal of emotional stimuli impact cognitive-motor performance in an oddball task. *Biological Psychology, 125*, 105–114.

Martini, N., Menicucci, D., Sebastiani, L., Bedini, R., Pingitore, A., Vanello, N., et al. (2012). The dynamics of EEG gamma responses to unpleasant visual stimuli: From local activity to functional connectivity. *Neuroimage, 60*(2), 922–932.

McAuley, J. H., Rothwell, J. C., & Marsden, C. D. (1997). Frequency peaks of tremor, muscle vibration and electromyographic activity at 10 Hz, 20 Hz and 40 Hz during human finger muscle contraction may reflect rhythmicities of central neural firing. *Experimental Brain Research, 114*(3), 525–541.

Minami, S., & Amano, K. (2017). Illusory jitter perceived at the frequency of alpha oscillations. *Current Biology, 27*(15) 2344-2351 e2344.

Mini, A., Palomba, D., Angrilli, A., & Bravi, S. (1996). Emotional information processing and visual evoked brain potentials. *Perceptual and Motor Skills, 83*(1), 143–152.

Morris, J. S., Ohman, A., & Dolan, R. J. (1998). Conscious and unconscious emotional learning in the human amygdala. *Nature, 393*(6684), 467–470.

Morris, J. S., Ohman, A., & Dolan, R. J. (1999). A subcortical pathway to the right amygdala mediating "unseen" fear. *Proceedings of the National Academy of Sciences of the United States of America, 96*(4), 1680–1685.

Muller, M. M., Keil, A., Gruber, T., & Elbert, T. (1999). Processing of affective pictures modulates right-hemispheric gamma band EEG activity. *Clinical Neurophysiology, 110*(11), 1913–1920.

Nasrallah, M., Carmel, D., & Lavie, N. (2009). Murder, she wrote: Enhanced sensitivity to negative word valence. *Emotion, 9*(5), 609–618.

Noguchi, Y., Xia, Y., & Kakigi, R. (2019). Desynchronizing to be faster? Perceptual- and attentional-modulation of brain rhythms at the sub-millisecond scale. *Neuroimage, 191*, 225–233.

Ohman, A., Flykt, A., & Esteves, F. (2001). Emotion drives attention: Detecting the snake in the grass. *Journal of Experimental Psychology General, 130*(3), 466–478.

Olofsson, J. K., Nordin, S., Sequeira, H., & Polich, J. (2008). Affective picture processing: An integrative review of ERP findings. *Biological Psychology, 77*(3), 247–265.

Oya, H., Kawasaki, H., Howard, M. A., 3rd, & Adolphs, R. (2002). Electrophysiological responses in the human amygdala discriminate emotion categories of complex visual stimuli. *Journal of Neuroscience, 22*(21), 9502–9512.

Pelli, D. G. (1997). The VideoToolbox software for visual psychophysics: Transforming numbers into movies. *Spatial Vision, 10*(4), 437–442.

Pessoa, L. (2008). On the relationship between emotion and cognition. *Nature Reviews Neuroscience, 9*(2), 148–158.

Samaha, J., & Postle, B. R. (2015). The speed of alpha-band oscillations predicts the temporal resolution of visual perception. *Current Biology, 25*(22), 2985–2990.

Softky, W. R., & Koch, C. (1993). The highly irregular firing of cortical cells is inconsistent with temporal integration of random EPSPs. *Journal of Neuroscience, 13*(1), 334–350.

Tadel, F., Baillet, S., Mosher, J. C., Pantazis, D., & Leahy, R. M. (2011). Brainstorm: A user-friendly application for MEG/EEG analysis. *Computational Intelligence and Neuroscience, 2011*, 879716.

Taube, J. S. (2010). Interspike interval analyses reveal irregular firing patterns at short, but not long, intervals in rat head direction cells. *Journal of Neurophysiology, 104*(3), 1635–1648.

Woodruff, C. C., Barbera, D., & Von Oepen, R. (2016). Task-related dissociation of EEG beta enhancement and suppression. *International Journal of Psychophysiology, 99*, 18–23.

Wutz, A., Melcher, D., & Samaha, J. (2018). Frequency modulation of neural oscillations according to visual task demands. *Proceedings of the National Academy of Sciences of the United States of America, 115*(6), 1346–1351.

Wyart, V., & Tallon-Baudry, C. (2008). Neural dissociation between visual awareness and spatial attention. *Journal of Neuroscience, 28*(10), 2667–2679.

Zhu, M., Luo, J., Zhao, N., Hu, Y., Yan, L., & Gao, X. (2016). The temporal primacy of self-related stimuli and negative stimuli: An ERP-based comparative study. *Social Neuroscience, 11*(5), 507–514.